A 4 x 4 Low-Profile Hybrid Fed Antenna Array for Satellite Communication Applications

Ngoc-Lan Nguyen*[1]
[1]Wireless Communication Laboratory,
Posts and Telecommunications Institute of Technology, Ho Chi Minh City, Vietnam
HoChiMinh city, VietNam
Email: lannn@ptit.edu.vn

***Abstract* – A 4 × 4 broadband patch antenna array has been developed for satellite communication downlink within the 3.7–4.2 GHz frequency range. The proposed design utilizes a hybrid feeding network combining both parallel and series configurations. In which, T-junction power splitters are employed to distribute equal power to each vertical sub-array, while quarter-wavelength transformers provide impedance matching between series elements. Fabricated on a 1.575 mm-thick Rogers 4350B substrate, the overall dimensions of the fabricated prototype are $2.11\lambda_o \times 2.35\lambda_o \times 0.018\lambda_o$, where λ_o is the free-space wavelength at the lowest frequency. Measurement results show that the array achieves a −10 dB impedance bandwidth of 16.3%, a peak realized gain of 14.5 dBi at 3.8 GHz, and an efficiency above 68% across the operating range of frequency. These features show the proposed antenna is a strong candidate for satellite communication systems for broadband applications.**

Index Terms: Array antenna, series fed, satellite communication, microstrip patch antenna.

I. INTRODUCTION

The rapid development of satellite communication systems has increased the demand for compact, high-gain, and broadband antenna arrays that can support high data throughput and maintain stable downlink performance [1]. Planar microstrip antenna arrays are consistently popular choices because they offer a low-profile design, lightweight construction, and are easy to fabricate and integrate with RF circuits [2]. However, traditional microstrip antennas typically exhibit limited impedance bandwidth and low gain, which restricts their suitability for modern broadband satellite systems. To overcome these problems, approaches for different feed networks are investigated including series-fed [3], [4], [5], [6], parallel-fed arrays [7], [8], and combination (both series and parallel feeding) [9]. In [3], a novel method for designing series-fed patch antenna arrays is introduced. By utilizing the technique of series-feeding which the impedance matching can be implemented by controlling the inset position of the feeding line, this method not only reduces sidelobe levels, but also contributes to bandwidth enhancement. Consequently, a 12-element series-fed patch antenna array operating at 24 GHz was designed, simulated, and fabricated, achieving a sidelobe level (SLL) of 20 dB. The proposed design also expands the bandwidth from 1.7% to 2.5% and enhances radiation efficiency by 7%. Similarly, the authors in [4] employ multiple series-fed microstrip comb-line structures to develop linear arrays consisting of 8, 16, and 64 elements. The arrays work in the ISM band of 24 -24.25 GHz, achieving the peak values of gain of 12.2 dBi, 15 dBi, and 19.8 dBi, respectively, with low sidelobe levels, below -28 dB. The series-fed technique has also been utilized in the designs presented in [5], [6] to enhance the performance for antenna. Meanwhile, in [7], thanks to the presence of frequency selective surface (FSS) and parallel feeding, the antenna array 4 x 4 shows an impedance bandwidth at -10 dB of 36% and a peak gain of 15.1 dBi. This parallel feeding technique is also applied for an antenna including 64 elements yielding at 28 GHz for 5G applications [8]. The measured results exhibit a percentage of bandwidth at -10 dB and a peak gain are 11.1% and 23.5 dBi, respectively. Combining parallel and series feeding structures provides an effective means of improving the overall performance of an antenna array. Parallel-fed networks are appreciated for their relatively wide impedance bandwidth, yet they may experience gain reduction due to losses accumulating along the feed lines. In contrast, series-fed configurations generally incur lower distribution losses [10]. For these reasons, the methodology adopted in [9] is built upon this type of feeding architecture, where a 4 × 4 array is designed on a Rogers RT/Duroid 5880 substrate at the center frequency of 8.15 GHz. The final design with an overall size of $2.73\lambda_o \times 2.73\lambda_o \times 0.082\lambda_o$ delivers a 15.9% bandwidth and a peak gain of 20 dBi. Despite these advancements, the designs in [3], [4], [5], [6], and [8] are limited by narrow bandwidths (below 11.5%), while the large physical sizes remain a drawback in the works of [7] and [9].

In this paper, a 4 × 4 antenna array designed for satellite applications at a center frequency of 3.95 GHz is presented. By employing a hybrid feeding technique that combines series and parallel configurations, the measured impedance bandwidth reaches 17%, with a peak gain of 14.5 dBi. The antenna exhibits a planar, low-profile structure and broadband characteristics, validated through both Computer Simulation Technology (CST) Studio simulations and experimental measurements.

II. DESIGN OF ANTENNA

A. Single element

The progress of antenna development started with the design of a single element, with its structure depicted in Fig. 1. The microstrip patch antenna is chosen in this paper because of owning the characteristics such as low profile and ease of

fabrication, which are suitable for compact wireless systems. The antenna is implemented based on a Rogers 4350B substrate, with a thickness of 1.524 mm, a relative permittivity (ε_r) of 3.66, and a loss tangent ($tan\delta$) of 0.0037. Among various feeding techniques available for microstrip antennas, such as coaxial probe [11], aperture coupling [12], and microstrip line [13], the microstrip line feed is adopted in this work owing to its simplicity for both fabrication and impedance matching. The impedance matching can be achieved by adjusting the position of feeding along the patch. The design and simulation of the antenna are implemented by using the CST Studio software. After parametric optimization, the finalized geometrical parameters of the single antenna element are determined as follows: $W = 40$, $L = 35$, $w_p = 29$, $l_p = 20.5$, $c = 7$, $l_s = 8$, $w_s = 1.3$, $w_f = 3.3$, $l_f = 10$ (unit: *mm*). Fig. 2 exhibits the simulated $|S_{11}|$ and gain of the single element. As seen, the presented antenna achieves a -10 dB impedance bandwidth of 41 MHz, from 3.891 GHz to 3.932 GHz and a peak gain of 4.15 dBi observed at 3.92 GHz.

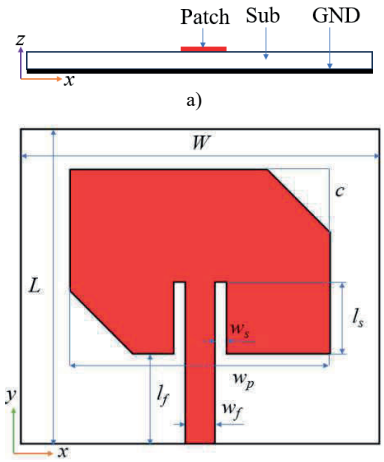

Fig. 1. The geography of single element: (a) cross-section view, (b) patch element

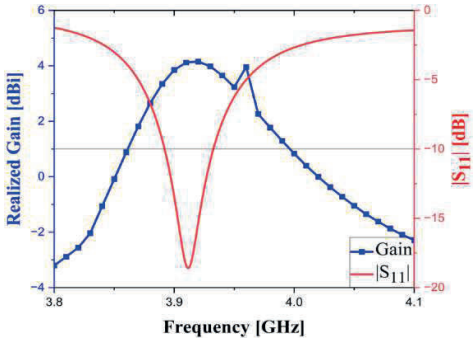

Fig. 2. |S11| and gain of the single element

B. Power Divider

In antenna array configurations, power dividers play a vital role in power distribution from a common source to multiple radiating elements. Currently, various kinds of power dividers are introduced, for example: T-junctions [14], Wilkinson [15], and hybrid [16]. Each type has its own characteristics. Because of owing the features such as structural simplicity and low insertion loss, T-junction dividers are selected in this design. The T-junction power divider is a basic three-port passive network. Depending on design requirements, an arbitrary power division ratio can be achieved. In this study, an equal-split configuration is implemented, delivering in-phase output signals with a -3 dB power division at each output port. The geometric configuration and key characteristics of the power divider are adopted in Fig. 3. The final parameters after optimization are as follows (in mm): $W_s = 60$, $L_s = 40$, $w_t = 5.6$, $l_t = 13$, $w_d = 3.3$, $l_d = 12$, $c_d = 2.5$. As observed, the simulated results show that both $|S_{21}|$ and $|S_{31}|$ are approximately -3 dB, i.e., the power level at ports 2 and 3 is equal. In addition, the reflection coefficient at port 1 ($|S_{11}|$) remains below -15 dB in the operating band of frequency and this displays the good impedance matching of the input.

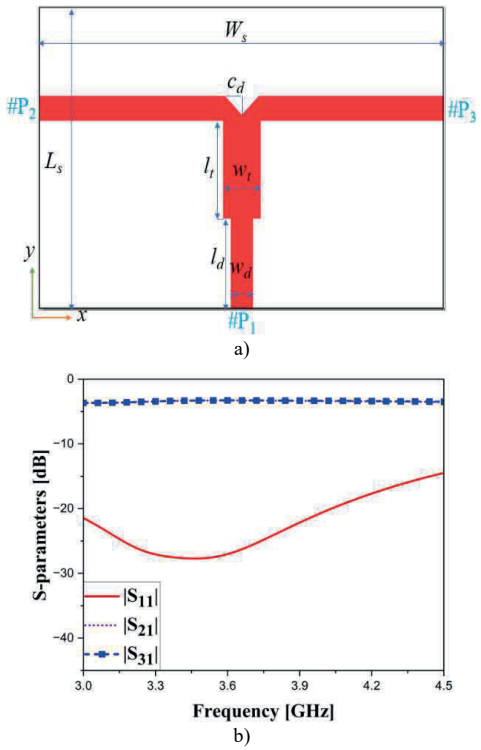

Fig. 3. The model (a) and its performance (b) of the power divider

C. Array Antenna

Based on the architecture of an antenna element, an antenna array configuration is subsequently analyzed. The detailed layout of the array is depicted in Fig. 4. This proposed design comprises 16 elements arranged in an array of 4 x 4, with the distance between elements along the x- and y-axes of 39 mm and 37 mm, respectively. To realize the power distribution and match impedance, transformers of quarter-wavelength impedance were utilized. The final proposed design has been optimized with the following dimensions: $W_a = 180$, $L_a = 200$, $w_e = 27$, $l_e = 22$, $l_o = 20$, $l_{fa} = 12$, $l_s = 6$, $c_a = 6$, $D_x = 39$, $D_y = 37$, $l_i = 6$, $w_i = 0.75$, $w_s = 1$, $w_t = 5.6$, $l_t = 11$, $l_f = 12$.

To better understand about the optimization process for antenna, some key parameters are investigated such as the patch element's width (w_e) and length (l_e), and the length of the quarter-wavelength impedance transformer (l_t). As illustrated in Fig. 5(a), a patch length (l_e) of 22 not only achieves the broadest

impedance bandwidth, but also remains the most stable gain value. When the patch length (l_e) increases to 24, the resonant frequency is moved to a lower side. Conversely, reducing the patch length (l_e) to 20 results in an upward frequency shift. These results are consistent with the theory.

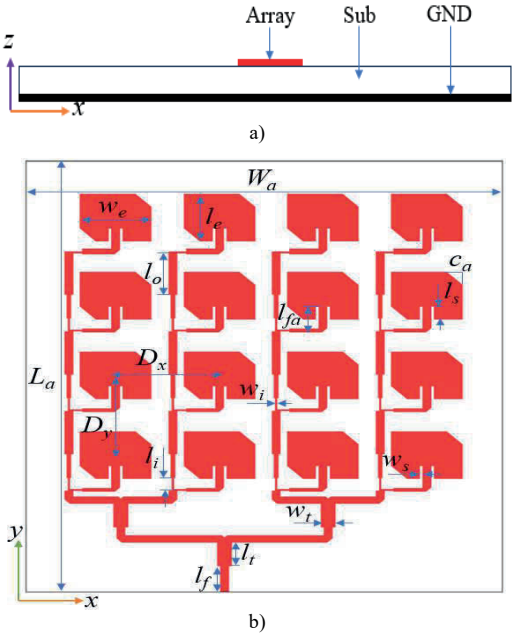

Fig. 4. The geometry of the proposed antenna: (a) cross-section view, (b) antenna array

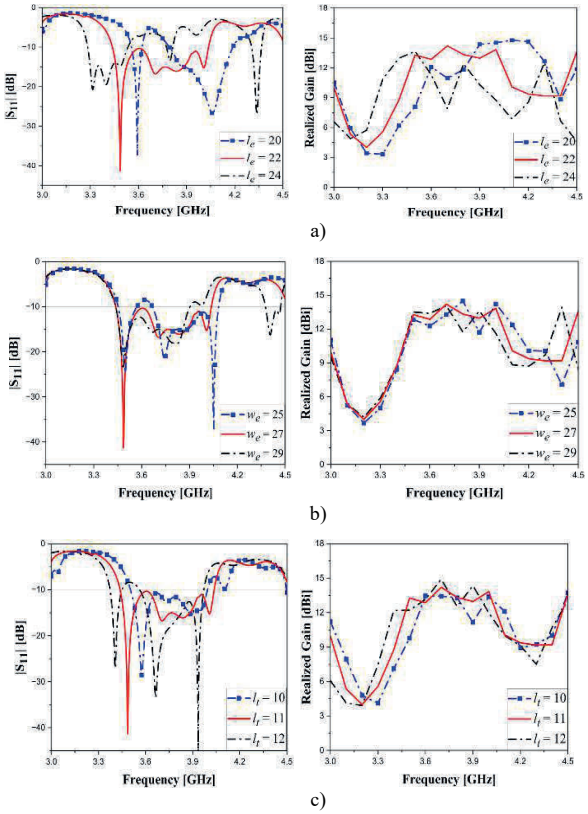

Fig. 5. $|S_{11}|$ (left) and gain (right) analysis for different (a) length of patch element (l_e), (b) width of patch element (w_e), and (c) length of quarter-wavelength impedance transformer (l_t).

Moving to Fig. 5(b), it can be seen that although a patch width (w_e) of 25 offers the widest bandwidth, the impedance matching is not good at 3.6 GHz (higher than -10 dB). In contrast, when w_e = 29, the bandwidth becomes the narrowest among the considered cases. Regarding the gain, although the gain value reaches maximum at w_e = 25, its fluctuation over the operating band of frequency is significant. Meanwhile, in the 3.4 - 4.1 GHz range, the most stable value of gain is obtained when w_e = 27.

Switch to Fig. 5(c), the effect of wavelength transformer length (l_t) on antenna performance is implemented. The decrease in l_t results in a downward shift of the resonance frequency, whereas an increase in l_t leads to an upward shift. Additionally, for l_t = 12, the reflection coefficient exceeds −10 dB between 3.45 and 3.55 GHz, indicating degraded performance. In contrast, l_t = 11 provides both high and stable gain within the desired 3.4 - 4.1 GHz band.

III. FABRICATION AND MEASUREMENT

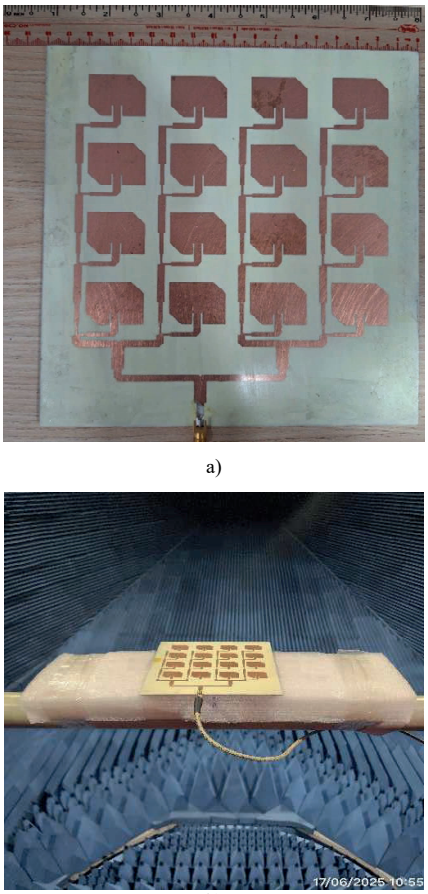

Fig. 6. The photograph of the fabricated prototype (a) and measurement setup (b)

To validate the proposed design concept, experimental measurements were performed on a fabricated prototype. A photograph of the realized antenna is provided in Fig. 6, whereas Fig. 7 compares the simulated and measured S-parameters, demonstrating the antenna's performance. The S-parameter was recorded using a Keysight E5071C network analyzer (100 kHz - 8.5 GHz). Radiation patterns were

measured in an MVG Orbit anechoic chamber with a Keysight N5222A PNA, while a calibrated horn antenna was employed as the gain reference.

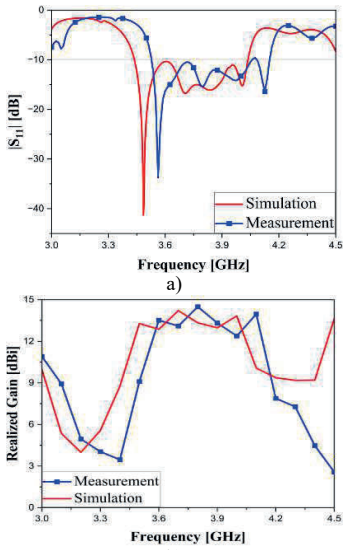

Fig. 7. Measured and simulated results: (a) |S11|; (b) Realized Gain

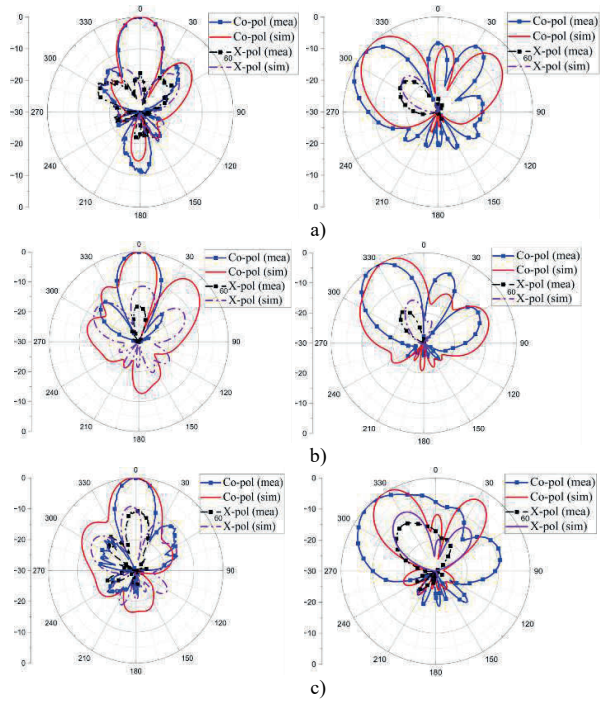

Fig. 8. Simulated and measured radiation patterns in x-z (left) and y-z (right) planes of the proposed antenna array at: (a) 3.6 GHz, (b) 3.8 GHz, and (c) 4 GHz

A similar behavior is observed between the simulated and measured results. For the simulated case, the −10 dB impedance bandwidth is 3.43-4.03 GHz, corresponding to 15.8%, whereas the measured bandwidth extends from 3.53 - 4.15 GHz, equivalent to 16.3%. Within these respective frequency ranges, the gain varies between 8.7–14.21 dBi for simulation and 9.1–14.5 dBi for measurement. The maximum values of gain for simulation and measurement are 14.21 dBi at 3.7 GHz and 14.5 dBi at 3.8 GHz, respectively. There is a minor frequency shift between these two datasets. This could be because of (i) tolerances in fabrication, (ii) insertion loss of the SMA connectors, or (iii) imperfections in the chamber. Although there are these differences, the overall agreement between the simulation and the measurement is seen as acceptable.

Figure 8 shows the radiation patterns at 3.6 GHz, 3.8 GHz, and 4.0 GHz. It is evident that the simulated and measured results demonstrate consistent trends. The main lobe's deviation in the y-z plane from the 0° direction is caused by series feeding, which causes a phase difference between the array elements.

Table 1 gives a comparison in performance between the proposed design and other recent works. The proposed design has the highest fractional bandwidth of all the compared designs. Moreover, the antennas presented in [8] and [9] not only exhibit low gain, but also their dimensions are still quite. In contrast, this work achieves a good balance between important performance metrics. The proposed antenna is a promising candidate for practical application because it has a broadband feature and a small size.

TABLE I. COMPARATIVE PERFORMANCE ANALYSIS BETWEEN THE PROPOSED DESIGN AND RECENTLY REPORTED ANTENNAS

Ant	Freq [GHz]	Array size	BW [%]	Peak gain [dBi]	Total. Eff [%]	Size [λ^3]
[3]	24	12	2.5	16	81	N/G
[4]	24.125	16	1%	15	N/G	N/G
[5]	5.76	9	1.5	12.8	N/G	N/G
[8]	30	64	11.1	23.5	79.4	7.2 × 7.7 × N/G
[9]	8.15	16	15.9	20.3	86.5	2.73 × 2.73 × 0.08 2
This work	**3.8**	**16**	**16.3**	**14.5**	**68**	**2.11 × 2.35 × 0.01 8**

IV. CONCLUSION

This paper describes a low-profile, broadband antenna designed for satellite communication applications in the 3.7 to 4.2 GHz frequency range. The antenna configuration includes 16 patch radiating elements arranged into a 4 x 4 array. The broadband feature is achieved by using a hybrid feeding scheme that combines both series and parallel connections. To validate the design concept, the fabricated prototype, which is 180 × 200 × 1.524 mm³ (2.11λ × 2.35λ × 0.018λ), has a −10 dB fractional bandwidth of 16.3%, a peak gain of 14.5 dBi, and maintains radiation efficiency above 68% across the desired frequency

range. Because of this combination of wide bandwidth and low profile, the proposed design has a lot of potential for use in real satellite communication systems.

ACKNOWLEDGMENT

This research is supported by Posts and Telecommunications Institute of Technology (PTIT).

REFERENCES

[1] S. Gao, Y. Rahmat-Samii, R. E. Hodges, and X. X. Yang, "Advanced Antennas for Small Satellites," *Proc. IEEE*, vol. 106, no. 3, pp. 391–403, 2018, doi: 10.1109/JPROC.2018.2804664.

[2] F. E. M. Tubbal, R. Raad, and K. W. Chin, "A survey and study of planar antennas for pico-satellites," *IEEE Access*, vol. 3, pp. 2590–2612, 2015, doi: 10.1109/ACCESS.2015.2506577.

[3] L. L. Hao Yi, Yajie Mu, Jiaqi Han, "Improved bandwidth and radiation efficiency of series-fed patch array using cascaded inset-fed mechanism," *Electron. Lett.*, vol. 58, pp. 866–868, 2022, doi: 10.1049/ell2.12641.

[4] J. Qian, H. Zhu, M. Tang, and J. Mao, "A 24 GHz Microstrip Comb Array Antenna with High Sidelobe Suppression for Radar Sensor," *IEEE Antennas Wirel. Propag. Lett.*, vol. 20, no. 7, pp. 1220–1224, 2021, doi: 10.1109/LAWP.2021.3075887.

[5] R. Chopra and G. Kumar, "Series-Fed Binomial Microstrip Arrays for Extremely Low Sidelobe Level," *IEEE Trans. Antennas Propag.*, vol. 67, no. 6, pp. 4275–4279, 2019, doi: 10.1109/TAP.2019.2908108.

[6] R. Chopra and G. Kumar, "Series- And Corner-Fed Planar Microstrip Antenna Arrays," *IEEE Trans. Antennas Propag.*, vol. 67, no. 9, pp. 5982–5990, 2019, doi: 10.1109/TAP.2019.2922774.

[7] N.-L. Nguyen *et al.*, "A Stacked Planar Antenna Array with Frequency Selective Surface for Downlink Applications of Small Satellites," *IETE J. Res.*, vol. 70, no. 7, pp. 6115–6123, 2024, doi: 10.1080/03772063.2023.2297385.

[8] E. R.-I. Carlos Sánchez-Cabello, Luis Fernando Herrán, Ashraf Uz Zaman, "Ka band microstrip fed slot array antenna with PMC packaging," *IET Microwaves, Antennas Propag.*, vol. 14, no. 14, pp. 1837–1845, 2020, doi: 10.1049/iet-map.2020.0565.

[9] S. X. Ta, V. Du Le, K. K. Nguyen, and C. Dao-Ngoc, "Planar circularly polarized X-band array antenna with low sidelobe and high aperture efficiency for small satellites," *Int. J. RF Microw. Comput. Eng.*, vol. 29, no. 11, pp. 1–9, 2019, doi: 10.1002/mmce.21914.

[10] H. Wang, K. E. Kedze, and I. Park, "Microstrip Patch Array Antenna Using a Parallel and Series Combination Feed Network," in *International Symposium on Antennas and Propagation (ISAP)*, Busan, Korea: IEEE, 2018, pp. 669–670.

[11] K. W. Leung, K. Y. A. Lai, K. M. Luk, and D. Lin, "Theory and Experiment of a Coaxial Probe Fed Hemispherical Dielectric Resonator Antenna," *IEEE Trans. Antennas Propag.*, vol. 41, no. 10, pp. 1390–1398, 1993, doi: 10.1109/8.247779.

[12] D. Anandkumar and R. G. Sangeetha, "Design and analysis of aperture coupled microstrip patch antenna for radar applications," *Int. J. Intell. Networks*, vol. 1, no. April, pp. 141–147, 2020, doi: 10.1016/j.ijin.2020.11.002.

[13] N. L. Nguyen, C. D. Bui, and Q. S. Nguyen, "Design of a compact antenna with broadband and high gain," *Electromagnetics*, vol. 44, no. 1, pp. 18–31, 2024, doi: 10.1080/02726343.2023.2300840.

[14] E. Saenz, A. Cantora, I. Ederra, R. Gonzalo, and P. De Maagt, "A metamaterial T-junction power divider," *IEEE Microw. Wirel. Components Lett.*, vol. 17, no. 3, pp. 172–174, 2007, doi: 10.1109/LMWC.2006.890447.

[15] J. C. Kao, Z. M. Tsai, K. Y. Lin, and H. Wang, "A modified wilkinson power divider with isolation bandwidth improvement," *IEEE Trans. Microw. Theory Tech.*, vol. 60, no. 9, pp. 2768–2780, 2012, doi: 10.1109/TMTT.2012.2206402.

[16] M. Zafar, S. Ekpo, J. George, P. Sheedy, M. Uko, and A. Gibson, "Hybrid Power Divider and Combiner for Passive RFID Tag Wireless Energy Harvesting," *IEEE Access*, vol. 10, pp. 502–515, 2022, doi: 10.1109/ACCESS.2021.3138070.